

Launch and deployment of distributed small satellite systems[☆]

N.H. Crisp^{*}, K. Smith, P. Hollingsworth

School of Mechanical, Aerospace and Civil Engineering, The University of Manchester, George Begg Building, Sackville St, Manchester M13 9PL, United Kingdom



ARTICLE INFO

Article history:

Received 4 November 2014

Received in revised form

14 April 2015

Accepted 18 April 2015

Available online 29 April 2015

Keywords:

Small satellites

Constellation deployment

Nanosatellite

CubeSat

Nodal precession

Earth–Moon Lagrange point L_1

ABSTRACT

The rise in launch and use of small satellites in the past decade, a result of improved functionality through technology miniaturisation and alternative design philosophies, has spawned interest in the development of distributed systems or constellations of small satellites. However, whilst a variety of missions based on constellations of small satellites have been proposed, issues relating to the launch and deployment of these distributed systems mean that few have actually been realised. A number of strategies have been proposed which enable multiple small satellites comprising a constellation to be launched together and efficiently separated on-orbit, thus reducing the total cost of launch. In this paper, two such strategies which have the potential to significantly increase the viability of small satellite constellations in Earth orbit are investigated. Deployment using natural Earth perturbations to indirectly achieve plane separations is analysed using a developed method and compared to deployment utilising the Earth–Moon Lagrange point L_1 as a staging area prior to return to LEO. The analysis of three example missions indicates that these two strategies can facilitate the successful establishment of small satellite constellations in Earth orbit whilst also reducing propulsive requirements, system complexity, and/or cost. The study also found that the method of nodal precession is sensitive to the effects of orbital decay due to drag and can result in long deployment times, and the use of Lunar L_1 is more suitable for constellation configurations where several satellites are present in each orbital plane.

© 2015 IAA. Published by Elsevier Ltd. on behalf of IAA. This is an open access article under the CC BY license (<http://creativecommons.org/licenses/by/4.0/>).

1. Introduction

A growing interest in the use of distributed systems or constellations of small satellites has been generated following the rise in popularity of small satellites, especially in the past decade. This growth in the use of small satellites has

been primarily driven by the miniaturisation of electronics and sensors [1] and the availability of commercial-off-the-shelf components with increasing capability, significantly reducing the cost of hardware development. The access-to-orbit and economy of these spacecraft is also improved through availability of secondary payload launch opportunities [2,3], especially for small satellites which conform to standardised form factors such as CubeSat [4].

In recent years, the launch of successful small satellite missions, particularly nanosatellites, with valuable engineering/technology demonstration (e.g. CanX-6/NTS [5], STRaND-1 [6]), scientific (e.g. O/OREOS [7], GeneSat-1 [8]), military (e.g. SMDC-One [9], SENSE-1), and commercial

[☆] This paper was presented during the 65th International Astronautical Congress in Toronto.

^{*} Corresponding author.

E-mail addresses: nicholas.crisp@manchester.ac.uk (N.H. Crisp), kate.smith@manchester.ac.uk (K. Smith), peter.hollingsworth@manchester.ac.uk (P. Hollingsworth).

(e.g. WNISAT-1 [10]) capabilities has now demonstrated the utility of this class of spacecraft in independent operation.

The use of small satellites in constellations has also been successfully demonstrated by a number of microsatellite-class missions, including the Disaster Monitoring Constellation (DMC) and RapidEye Earth observation missions and the ORBCOMM [11] satellite communications system.

The demonstration of small platform capability and constellation operation has recently resulted in the generation of larger multi-plane constellations of smaller satellites. Two such examples of this new generation of small satellite constellation are the Planet Labs [12] (Flock-1a: 28 satellites, Flock-1c: 11 satellites) and Skybox Imaging (24 satellites) Earth observation constellations which are currently in the process of being launched.

A further value proposition of small satellite constellations, resulting from their lower cost of platform development, is the ability to be launched in larger numbers and perform many simultaneous and distributed measurements or observations. A key feature of multi-plane systems of these satellites is increased temporal resolution of collected data (i.e. shorter revisit times) over single-plane or *string-of-pearls* configurations. Furthermore, the presence of multiple satellites in each orbital plane can facilitate a more graceful degradation of system performance on the occasion of individual satellite failures [13].

A variety of novel missions benefiting from these capabilities have been proposed in the fields of meteorology [14]; climate-science [14,15]; disaster warning and detection [16–18]; atmospheric, magnetospheric, and ionospheric measurement/observation [14–17,19,20]; and gravity and other Earth sciences [15]. Multi-satellite interplanetary exploration missions and constellations in orbit about other central bodies utilising small satellites are also being considered [16,17,21].

However, the current launch paradigm of secondary payload manifesting of small satellites limits the ability of these constellations to be successfully deployed into orbit. In particular, the lack of control on launch schedule and destination orbit prohibits the use of multiple secondary launch opportunities by constellations which require accurately coordinated orbits and multi-plane configurations. This issue is further compounded by technology, mass, and volume constraints on propulsion system capability to maintain low development and manufacturing costs and comply with launch vehicle regulations. These constraints can be particularly restrictive for the smaller nanosatellite and picosatellite class platforms which are therefore typically limited in their ability to individually manoeuvre into their mission orbits [1,4,22].

In order to enable the cost-effective realisation of small satellite constellations a number of deployment strategies have been proposed which allow the launch of a complete multi-plane constellation on a single vehicle with satellite distribution occurring on-orbit. Currently, the FORMOSAT-3/COSMIC mission is the only example of a multi-plane small satellite constellation to be deployed from a single launch vehicle.

This paper investigates two deployment methods for constellations with multi-plane configurations and the

ability of these methods to facilitate the establishment of these systems in low Earth orbit (LEO). Through the use of a developed methodology, described in detail in Section 4, the relative effectiveness of deployment using natural Earth perturbations and the Earth–Moon Lagrange point L_1 are considered for different constellation missions.

2. Launch of small satellites

The absence of sufficiently small or inexpensive launch vehicles for the delivery of small satellites to orbit presents a significant barrier to the development of small satellite missions given their typically smaller budgets and development time-scales. This issue of access-to-orbit is somewhat addressed by secondary payload launch opportunities, where satellite operators can either share launch vehicle capacity through clustering or rideshare agreements, or utilise excess capacity on a commissioned launch of a larger satellite, a practise termed piggybacking. Unless arranged through a launch programme (e.g. NASA CubeSat Launch Initiative and Educational Launch of Nanosatellites) with provided or subsidised launch, the cost of secondary payload opportunities is generally greater than the specific cost (\$/kg) of the launch vehicle itself [23]. However, these opportunities still allow small payloads to achieve access-to-orbit at a significantly lower total expense than an independently commissioned launch.

The use of secondary payload opportunities is limited by the lack of control on the launch schedule and destination orbit of the vehicle, both controlled by the requirements of the primary payload or determined by a compromise between the payload operators in a rideshare launch. As a result, satellites launched as secondary payloads need to be flexible with regard to the orbit in which their mission can be performed. For some missions, this flexibility may not be feasible or may be too costly to embed in the system design.

Further restrictions on the launch of small satellites utilising secondary payload opportunities can include the requirement to be compatible with a certain class of deployment mechanism (e.g. P-POD, X-POD, ISIPOD), reducing the level of certification required by the secondary payloads by isolating them from the launch vehicle and primary payload [4]. This can further constrain the mass and volume of the satellite and any provision for deployable surfaces such as solar arrays or wireless communication antennae. Constraints on volumes and pressures of stored propellant, nominally to protect the primary payload, can also limit the capability of on-board propulsion systems, further restricting the ability of the secondary payloads to manoeuvre into more suitable or favourable mission orbits.

A number of new launch vehicles aiming to address the microsatellite and nanosatellite launch capability gap are currently in varying stages of development. The payload capability of these vehicles ranges from 12 to 300 kg with specific launch costs in the range of current secondary payload opportunities. Notable examples include the Virgin Galactic LauncherOne which will be air-launched from the White-KnightTwo carrier aircraft and will have a capacity on the order of 225 kg to LEO [24], a 10 kg payload launcher deployed from the XCOR Aerospace Lynx Mk.III suborbital

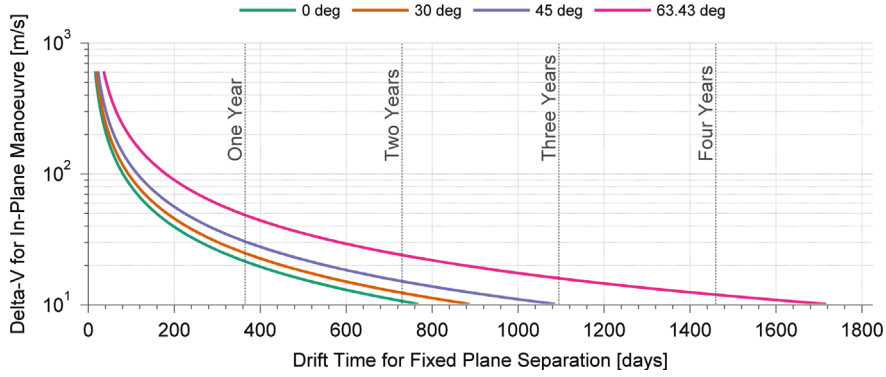


Fig. 1. Δv with drift time for a fixed plane separation of 60° at varying inclination.

vehicle [25], and the DARPA ALASA program involving several companies working towards the launch of a 45 kg payload to orbit for less than \$1M.

These vehicles will support the dedicated launch of microsattellites and nanosatellites, avoiding the potentially mission critical issues related to secondary payload launch opportunities.

2.1. Launch of small satellite constellations

Traditionally, constellations of satellites have been populated through many launches, one or more per orbital plane, or even one per satellite. However, due to the prohibitive cost of launch in comparison to the development cost of smaller satellites, launch in this manner is not economically viable for small satellite constellations.

For relatively high-budget missions of microsattelite constellations, the cluster launch method can currently provide the opportunity to launch a constellation to orbit. For example, the FORMOSAT-3/COSMIC mission of five ~ 61 kg satellites was launched on an Orbital Sciences Minotaur I vehicle [26]. However, due to the present lack of sufficiently small launch vehicles, the launch of similar nanosatellite and picosatellite constellations, unless in extremely large numbers, becomes uneconomical. The launch of a very small satellite constellation, the Planet Labs Flock constellation of 3U CubeSats, has thus far achieved orbit by both manifestation on a re-supply launch to the ISS and subsequent deployment from the Kibo module and deployment as secondary payloads from a Dnepr launch, resulting in different orbital inclinations and altitudes [12].

The emergence of new small launch vehicles, mentioned previously, would support the cluster launch of very small satellite constellations.

3. Constellation deployment strategies

For many missions a fixed constellation configuration of the payloads is required. If many small satellites comprising a constellation are launched from a single launch vehicle, the payloads must be dispersed on-orbit into their respective mission orbits. However, to reduce system complexity and development costs, if present, the propulsion systems on-board these small platforms are typically limited in

capability. Further technological, mass and volume constraints can compound this issue. The ability of small satellites to simply manoeuvre from their insertion orbit into their required mission orbits is therefore restricted, especially if expensive out-of-plane manoeuvres in Right Ascension of Ascending Node (RAAN) or inclination are required.

In order to achieve the payload distribution required by the mission specification, various deployment strategies have been developed allowing multiple satellites to be launched together and separated on-orbit. These include the use of nodal precession due to natural Earth perturbations and the use of the Earth–Moon Lagrange point L_1 , which will be examined in Sections 3.1 and 3.2.

3.1. Nodal precession

A method of constellation deployment using natural orbital perturbations to separate orbital planes in RAAN, often termed *indirect plane separation*, was patented in 1993 by King and Beidleman [27]. The method utilises the differential rate of nodal precession due to the non-spherical geopotential of the Earth whereby orbits with different sizes, shapes, or orientation precesses at different rates, allowing plane separations to be achieved without out-of-plane manoeuvring. Eq. (1) [13] shows the analytical form for the rate of nodal precession $\dot{\Omega}$, as a function of semi-major axis a , eccentricity e , and inclination i . In Eq. (1), only the secular effects due to the second degree zonal harmonic J_2 are shown for brevity:

$$\dot{\Omega}_{J_2} = -\frac{3}{2} \cdot \frac{R_E^2}{(a(1-e^2))^2} \cdot J_2 \cdot n \cdot \cos i \quad (1)$$

The process for a constellation deployment from a common insertion orbit initially requires an in-plane manoeuvre of a satellite into an orbit with a different rate of nodal precession, nominally the mission orbit. A drift period is then required in order to achieve the correct angular separation in RAAN, before a second satellite is manoeuvred into the mission orbit, fixing the developed plane separation between the first two payloads. This process is repeated for all required planes in the constellation.

The drifting time required for such a deployment is dependent on the required separations and the differential drift rate between the initial and modified orbits, and is

therefore affected by the propulsive capability of the satellites. The relationship between time for a fixed plane separation and propulsive capability (Δv) for different orbital inclinations is shown in Fig. 1. For modest Δv expenditures, drift periods for the deployment of a complete constellation can be expected to be on the order of many months to years. These long drift-times may be undesirable from an operation or mission impact perspective or may present issues regarding the lifetime of the satellite in orbit with respect to both orbital decay and hardware reliability.

The deployment of multiple-satellites into each orbital plane can be facilitated by manifesting the payloads on carrier vehicles, termed pallets by King and Beidleman [27]. These carrier vehicles, each equipped with a centralised propulsion system, can perform the required manoeuvre and drift strategy to enter the correct orbital plane before releasing the individual satellites.

The benefit of a propulsion system common to a group of satellites is the alleviation of some mass and volume constraints. Some propulsion technologies which are not suitable for the individual satellite platforms due to size may also become viable due to the increased scaling of the system.

Finally, the satellites on each pallet can be distributed about the orbit in each plane. Aside from individual phasing of the payloads, this can be achieved using differential spring separation energies from the pallets, requiring a wait period of up to 50 days and a small Δv contribution from each satellite (up to 7.4 m s^{-1}) in order to freeze the distribution [28].

Differential drag methods can also be used to achieve required in-plane separations, demonstrated by the Aero-Cube-4 mission [29] and Planet Labs Flock-1 constellation [12] and proposed for use on the NASA CYGNSS mission due for launch in 2016 [30]. These systems use active attitude control methods and deployable surfaces to alter the projected area of the satellite and therefore drag profile to achieve minor differences in semi-major axis, therefore enabling the separation of the satellites within the plane.

This method of constellation deployment utilising differential nodal drift rates has thus far only been demonstrated by the FORMOSAT-3/COSMIC mission, launched in April 2006, in which 6 satellites were each deployed into a different plane [31]. A total Δv requirement of 147 m s^{-1} was estimated for each satellite, provided by multiple thrust-burns of the Hydrazine monopropellant propulsion subsystem. A total period of approximately 20 months was required for the deployment of this constellation.

3.2. Lunar L_1

A method of LEO constellation deployment utilising the first Earth–Moon Lagrange point (EML-1) was proposed by Chase et al. [32] and developed by Nadoushan and Novinzadeh [33]. In this method satellites for each intended plane of the constellation are manifested on carrier vehicles which are all launched together on a single vehicle to EML-1. The complement of carrier vehicles is inserted into a Halo orbit at EML-1 before being individually returned to Earth orbit with the required inclination (up to 60°) and ascending node. An aerocapture or aerobraking manoeuvre can be used to reduce the Δv

expenditure for Earth orbit re-entry. An aerocapture manoeuvre differs from aerobraking in that the total speed reduction is performed during only one pass through the atmosphere of the central body, utilising the high aerodynamic drag of an elliptical orbit with a low altitude perigee. Aerobraking manoeuvres utilise a higher altitude perigee with lower drag, therefore requiring more passes to bring the satellite into the correct orbit, but with lower aerodynamic forces and heating effects.

Following direct launch to EML-1 or transfer from LEO, the propulsive requirements of the carrier vehicles for deployment using this method involve manoeuvres for Halo orbit injection and departure at EML-1, approximately 600 m s^{-1} each, and Earth orbit circularisation after the aerocapture manoeuvre (120 m s^{-1}) [32,34]. Finally, phasing manoeuvres must be performed by the individual satellites in order to achieve the in-plane separations.

The primary benefit to this method of deployment is the significantly reduced time required in order to achieve the mission configuration whilst still enabling the use of a single launch. A period on the order of 20 days is required to return a complement of payloads to Earth orbit with any required spacing of the orbital planes in RAAN [33].

4. Analysis methods

The feasibility of these deployment methods for supporting missions of interest is primarily dependent on the time and energy required by the deployment strategy and the mission requirements of the constellation.

Deployment of LEO constellations by nodal precession requires consideration of the effects of atmospheric drag on the satellites. Satellites in orbits of a different semi-major axis and eccentricity can experience significantly different levels of drag and will therefore decay at different rates. For low altitude constellations, there may be a risk of satellite de-orbit before the deployment scheme has been completed. Propagation of the satellites throughout the deployment procedure can be used to determine the effect of drag on the constellation.

The physical characteristics of the satellites and optional carrier vehicles can also influence the deployment process, affecting the magnitude of drag experienced and propulsive system requirements. Additional system masses, such as aerocapture devices and payload deployment systems, must also be considered.

4.1. Satellite propagation

A semi-analytical propagation method developed by Liu and Alford [35], Semi-Analytical Liu Theory (SALT), was used in order to analyse the orbits of the satellites during the deployment of the constellation using the differential nodal precession method. Accommodation of both effects due to atmospheric drag and the non-spherical geopotential of the Earth are required in order to allow analysis in the LEO environment and determination of the rate of nodal precession of the orbits [36].

A semi-analytical method was chosen due to its speed of execution in comparison to numerical propagation techniques, allowing for the analysis of a potentially large

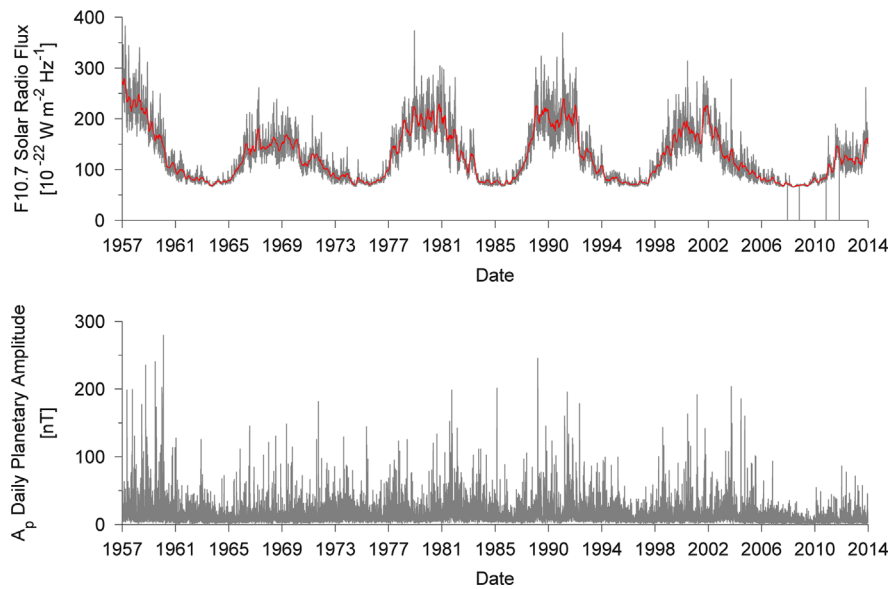


Fig. 2. Daily and 81-day centred average $F_{10.7}$ solar radio flux and daily planetary amplitude, A_p .

number of satellites over long time periods. Furthermore, the increased precision of a fully numerically determined solution would be dominated by the uncertainties associated with the evaluation of future atmospheric density using predicted solar flux and geomagnetic index data. In contrast to purely analytical methods, a semi-analytical propagation method can accommodate the use of a complex atmospheric density model rather than requiring a simplified model or series-expansion.

SALT uses a combination of both general and special perturbation techniques to consider both effects of atmospheric drag and perturbations due to non-spherical geopotential. Perturbations due to third body effects (lunar and solar) and solar radiation pressure are neglected due to their small magnitude in comparison to the primary perturbations and domination by the uncertainty involved in atmospheric density and ballistic coefficient determination [35].

The 2001 United States Naval Research Laboratory Mass Spectrometer and Incoherent Scatter Radar Exosphere (NRLMSISE-00) atmosphere model was used for density evaluation in the orbit propagator. The NRLMSISE-00 model is a global and time-varying model of the Earth's atmosphere valid from the ground to 1000 km altitude [37]. The required inputs to the model include longitude; geodetic altitude and latitude; date and time; A_p geomagnetic index; and daily and 81-day centred average $F_{10.7}$ Solar radio flux.

Whilst complex modern atmospheric density models can exhibit significant improvements over older techniques (e.g. 1976 Standard Atmosphere Extended, Exponential Model), a number of simplifications and assumptions are made in order to facilitate their development. As a result, significant errors are present in the evaluation of atmospheric density, typically in the range 10–20% [38].

For analysis of proposed missions, the evaluation of atmospheric density and drag is further complicated by

the requirement for forecast solar flux and geomagnetic index data. Due to the highly dynamic nature of the Sun and near-Earth environment these parameters are difficult to predict, and are therefore associated with a high level of uncertainty.

4.2. Space weather indices

Solar flux incident on the upper atmosphere of the Earth, primarily Extreme Ultraviolet (EUV) radiation, has a heating effect which affects the local atmospheric density. The variation of incident solar flux affects the level of heating within the atmosphere, and therefore the drag that a satellite in orbit will experience.

Measurements of solar flux with a wavelength of 10.7 cm ($F_{10.7}$) are used as a surrogate for EUV radiation due to their similar level of production by the Sun and low level of absorbance of $F_{10.7}$ in the atmosphere. Ground-based sensors can therefore be used to measure the level of incident $F_{10.7}$ on the Earth and approximate the effect of EUV on atmospheric density [36].

The level of $F_{10.7}$ has both a number of periodic trends and significant random variation, shown in Fig. 2. In the long term, $F_{10.7}$ varies with the 11-year solar cycle, leading to lengthy periods of high and low solar flux, solar maxima and minima. However, the magnitude and timing of the solar cycle is difficult to predict, leading to significant uncertainty in solar flux prediction. Furthermore, random variation in solar flux can be seen to increase during solar maxima in comparison to periods of solar minima. In the short-term, solar flux variability is primarily related to the 27-day rotation of the Sun, causing transient areas of high and low activity to turn towards or away from the Earth [36,39].

The prediction of geomagnetic index, a measurement of the interaction between energetic charged particles ejected from the Sun and atmospheric molecules, caus-

ing particle ionisation and a heating effect, is similarly complex. Geomagnetic index is expressed as either planetary index, K_p (on a scale of 0–9), or planetary amplitude a_p (0–400 nT), measured globally every 3 h. A daily planetary amplitude, A_p , is generated by averaging the set of 3-hourly a_p values. Due to the influence of the Sun, coupling with the solar cycle is present in the magnitude of geomagnetic index. The most pronounced effect is that variability increases somewhat during periods of solar maxima, shown in Fig. 2.

For the deployment of satellite constellations in LEO, the long-term forecasting of solar flux and geomagnetic index is critical due to the length of analysis required. A number of approaches used for the prediction of these indices are examined by Vallado and Finkleman [40] and Vallado and Kelso [41,42]. In Fig. 3, historic NOAA/SWPC predictions are shown against measured values. A polynomial trend developed by Vallado [36], matched to the magnitude and phasing of the past four solar cycles is also shown. The performance of these predictions show a capability to reasonably match the trend of solar flux through the remainder of a solar cycle. However, the predictions are typically incapable of matching the trend spanning multiple solar cycles. This is demonstrated by the performance of prediction of the latest solar cycle which has a characteristically lower magnitude and later occurrence of solar maximum.

The aggregated set of solar flux and geomagnetic index data from NOAA/SWPC, available from the *CelesTrak* website, was chosen due to the completeness and availability of up-to-date measured and forecast data.

4.3. Ballistic coefficient

The physical characteristics of orbiting satellites affect the amount of drag which is experienced whilst in orbit. The coefficient of drag C_D , spacecraft mass m , and cross-sectional area A can be mathematically combined to generate the ballistic coefficient for the satellite, Eq. (2), a measure of the effect of drag as a result of the physical

properties of the spacecraft:

$$BC = \frac{C_D A}{m} \quad (2)$$

Whilst the mass of a satellite is usually known or can be calculated from propellant usage, the evaluation of drag coefficient and cross-sectional area can be more complex.

The coefficient of drag for a spacecraft is both related to the shape of the spacecraft and the molecular interaction between atmospheric gas particles and the surfaces of the spacecraft. As a result, the coefficient of drag for the spacecraft can vary significantly with altitude due to the varying levels of atmospheric constituents [43]. However, for long analysis periods this variation in drag coefficient with altitude can be accounted for through the use of an average value, the classic estimate of 2.2 is typically used [44].

The cross-sectional area for ballistic coefficient determination is taken normal to the velocity vector of the satellite and is therefore dependent on the attitude of the spacecraft. If the attitude is known, either fixed or rotating, the cross-sectional area with respect to the velocity vector can be calculated. However, for tumbling spacecraft with constantly varying attitude, an averaged cross-sectional area can be calculated either by integrating the different cross-sectional areas over the range of possible attitudes or using a simplified flat-plate model [44].

4.4. Deployment analysis procedure

Utilising the principles set out in Sections 4.1–4.3, the deployment of a constellation of satellites using the method of differential nodal precession from a single launch insertion point can be analysed. The deployment analysis of a constellation with one satellite in each plane can be represented by the basic procedure shown in Fig. 4.

The semi-analytical propagation method enables the examination of satellite orbital decay through the use of predicted Earth environment data and a complex atmospheric density model. For constellations inserted or operated in low altitude orbits, the decay of satellites prior to the complete deployment of the constellation would

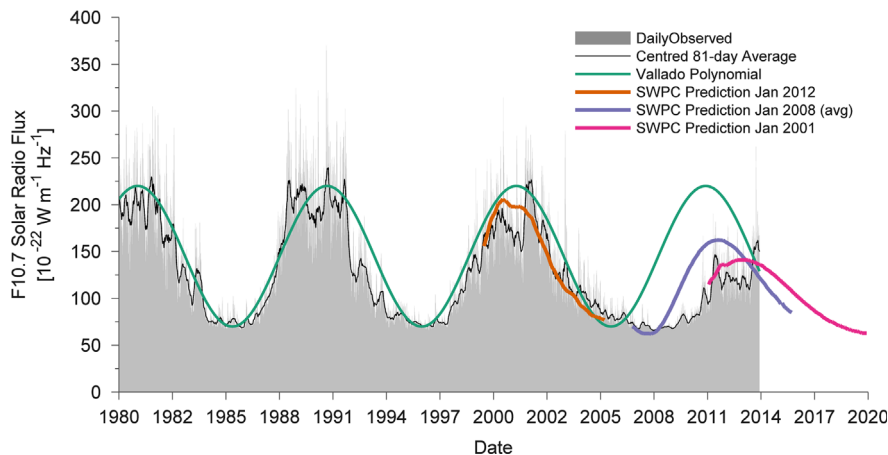


Fig. 3. Comparison of measured and predicted $F_{10.7}$ solar radio flux.

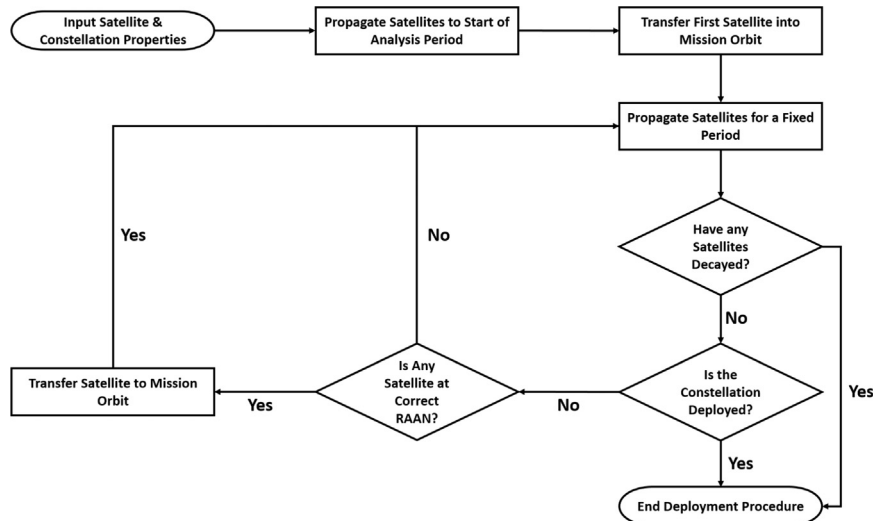


Fig. 4. Procedure for deployment analysis of a constellation with one satellite per plane.

constitute an infeasible design. Furthermore, any change in orbit shape and size alters the rate of nodal precession and can therefore affect the rate of separation of planes in the constellation.

For constellation configurations in which there is more than one satellite in each plane additional phasing manoeuvres are required to achieve the configuration of payloads. In these circumstances, carrier vehicles can be used in order to perform the more intensive in-plane manoeuvres and then dispense the payloads into each plane.

4.5. Analysis of Lunar L_1 deployment

Due to the complexity of trajectory design for missions involving EML-1, the corresponding analysis for deployment of constellations EML-1 for staging of return to LEO is treated in a more qualitative manner.

The first stage of an EML-1 deployment strategy requires either a launch vehicle capable of direct launch to EML-1 or transfer of payloads from LEO. Due to the relatively high Δv of transfer to EML-1 ($\sim 3.8 \text{ km s}^{-1}$), system complexity can be reduced by manifesting the payloads or sub-carrier vehicles on a single transfer vehicle with a capable and centralised propulsion system.

On the return to Earth orbit, aerocapture or aerobraking manoeuvres are required to reduce the velocity of the payloads or carrier vehicles. The use of ballute devices (inflated parachutes for high-speed aerodynamic braking) and drag-sails is typically proposed to perform these aerodynamic manoeuvres, significantly reducing the propulsive requirements of the system. However, additional mass, system complexity, and cost may be associated with the use of such devices and manoeuvres. Issues such as thermal shielding and additional structural requirements due to aerodynamic forces and heating, increased attitude control requirements, and radiation hardening of components due to passes through the van Allen belts must be considered if aerocapture or aerobraking manoeuvres are to be used.

Finally, the payloads or carrier vehicles must perform a re-circularisation manoeuvre for insertion into the mission orbit and any phasing manoeuvres required.

5. Constellation deployment analysis

The method of analysis for deployment using the method of indirect plane changes can be validated against the actual deployment of the FORMOSAT-3/COSMIC mission.

Analysis of other small satellite constellation missions with varying properties and configurations can be used to investigate the implementation of the different deployment methods and their relative capabilities and limitations.

5.1. Deployment of FORMOSAT-3/COSMIC

The FORMOSAT-3/COSMIC constellation of six micro-satellites was launched in April 2006 on an Orbital Sciences Minotaur vehicle. To achieve the mission configuration, the six payloads were deployed into six orbital planes equispaced about 180° in RAAN using the method of natural nodal precession over a period of 20 months.

As this mission has been launched and deployed, the actual deployment of the satellites, using Two-Line Element (TLE) data can be compared to the deployment simulated using the analysis technique previously detailed. The satellite platform properties, insertion orbit, and required mission orbits of the satellites are shown in Table 1. This information was used as the input variables for the deployment analysis. As only one satellite per plane was required by this constellation, no benefit to the deployment process could be gained through the use of carrier vehicles. Historical measured values for solar flux and geomagnetic activity were utilised in the propagation method.

Comparison of the semi-major axis and RAAN profiles of the actual mission, shown in Fig. 5, and the analytically determined deployment, shown in Fig. 6, indicates that the

developed analysis is capable of successfully characterising the process of constellation deployment using nodal precession. However, several discrepancies exist between the two data-sets which are due to mission changes, anomalies, and system failures in the actual deployment of the constellation:

- (a) The discontinuous orbit-raising of FORMOSAT-3F was caused by an intentional change in the specified plane spacing from 24° to 30° after the manoeuvre had begun. To enable the correct separation of all the orbital planes, an additional drift period was required before the manoeuvre could be completed.

- (b) The incomplete deployment of FORMOSAT-3D was due to a propulsion system malfunction which prohibited the satellite from achieving the correct mission orbit.
- (c) Numerous thrust-burn failures and an issue with thrusting during sunlit periods are also contributing factors to irregularities and discontinuities in the orbit-raising manoeuvres of the satellites during the deployment of the constellation.

Table 1

FORMOSAT-3/COSMIC mission specifications [31,26].

Property	Value
No. of satellites	6
No. of planes	6
Satellite dry mass	54 kg
Satellite fuel mass	6.65 kg
Thrust, BoL to EoL	1.1 N to 0.2 N
Specific impulse	217 s to 194 s
Satellite area	0.5963 m ²
Satellite C _D	2.2 (Assumed)
Insertion orbit	
Semi-major axis, a	6893 km
Eccentricity, e	0.00323
Inclination, i	71.992°
RAAN, Ω	301.158°
Mission orbit	
Semi-major axis, a_i	7178 km
Eccentricity, e_i	< 0.014
Inclination, i_i	71.992°
RAAN	$\Omega_1, \Omega_1 - (30, 60, 90, 120, 150)^\circ$

The calculated and actual Δv requirement of each satellite in the constellation is presented in Table 2 in order of satellite deployed. Given the same initial and final orbit, the difference in analytically calculated Δv between the satellites is due to the amount of orbital decay experienced. The satellites which stayed in the lower altitude initial orbit for longer experienced a greater level of drag for a longer period and therefore required a marginally larger orbit-raising manoeuvre to achieve the final mission orbit. The actual Δv values were calculated using the average increase in semi-major axis per burn and number of thrust events recorded for each satellite by Fong et al. [31]. The actual Δv expenditure calculated for FORMOSAT-3B using the published data appears to be incorrect, as this would not have been sufficient to raise the satellite from the insertion orbit to the mission orbit.

Aside from the propulsive failure for FORMOSAT-3D and an anomalistic value for FORMOSAT-3B, the difference between the predicted and actual Δv expenditure is less than 1%.

Deployment of the FORMOSAT-3/COSMIC mission using EML-1 can also be considered. However, due to the constellation configuration of only one satellite in each orbital plane, each platform would require an individual

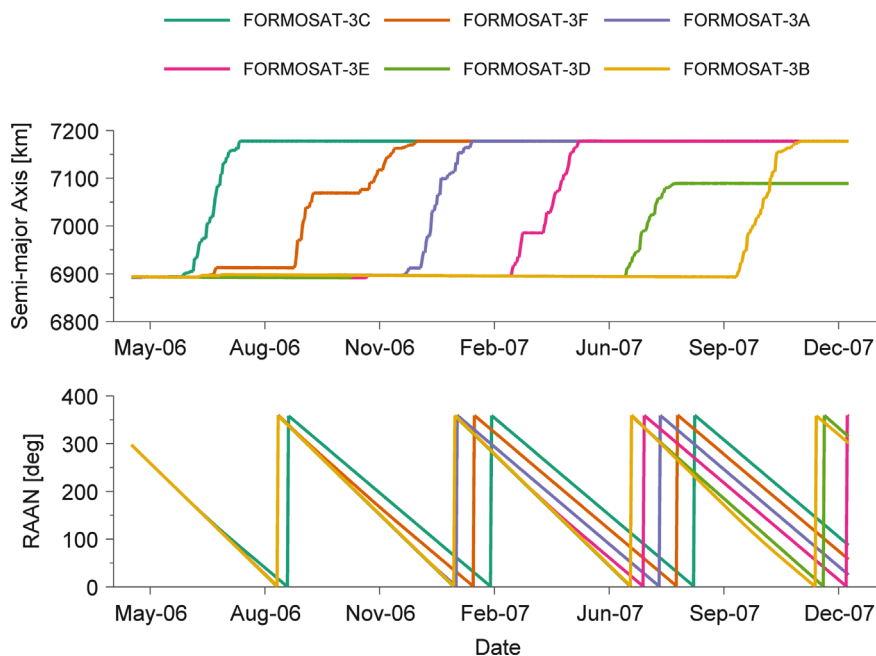


Fig. 5. Semi-major axis and RAAN of FORMOSAT-3/COSMIC mission from TLE data.

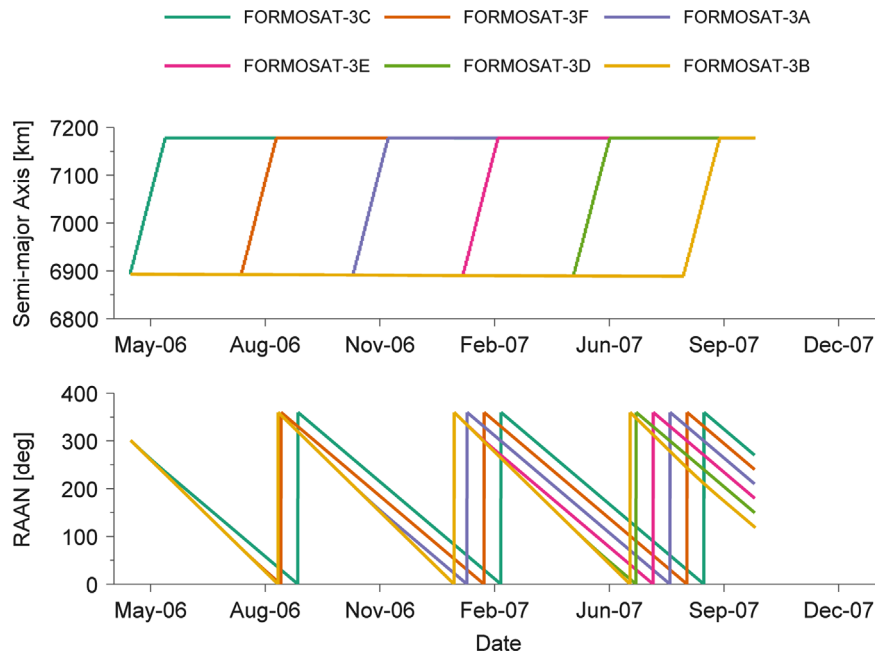


Fig. 6. Semi-major axis and RAAN of FORMOSAT-3/COSMIC mission using developed analysis.

Table 2

Calculated Δv requirement for FORMOSAT-3/COSMIC deployment.

Satellite	Analytical Δv (m s^{-1})	Actual Δv (m s^{-1}) [31]
3C (FM5)	152.2	153.1
3F (FM2)	152.6	154.0
3A (FM6)	153.0	153.0
3E (FM4)	153.7	154.0
3D (FM3)	154.1	107.9 ^a
3B (FM1)	154.5	129.8 ^b

^a Propulsion system failure

^b Minimum Δv for transfer is 152.1 m s^{-1}

ballute device ($\sim 50 \text{ kg}$ [34]) to perform the aerocapture procedure and a significantly more capable propulsion system to perform the Earth orbit re-circularisation and Halo orbit ejection manoeuvres.

The fuel mass to perform the required manoeuvres can be calculated using the rocket equation and an assumed dry mass of the system. For a bipropellant propulsion system with an I_{sp} of 300 s, the mass of propellant required for the total Δv of approximately 1500 m s^{-1} is $\sim 75 \text{ kg}$. This results in a total satellite wet mass in excess of 190 kg, over three times greater than the original payloads. Additionally, the delivery of these heavier payloads to EML-1 requires a greater launch capability, increasing costs further.

However, deployment of the constellation using transfer from EML-1 could be completed in a significantly reduced time compared to deployment performed using nodal precession which required a period of over 20 months. Should the establishment of the constellation been more urgent, deployment utilising EML-1 may have been the preferred method.

5.2. Halo constellation deployment

A number of novel and interesting configurations of small satellite constellations are proposed by Janson [45]. One of these constellations, termed a Halo constellation, is a Walker-Delta configuration in which a large number of payloads are equispaced about 360° in RAAN with no relative-phasing. This results in a 'bouncing' motion of the satellites, shown in Fig. 7 for a $60^\circ:50/50/0$ constellation at an altitude of 1000 km. For a constellation of this configuration the period of the bounce is 105.1 min [45]. Due to the fixed relationship between all the satellites in the constellation, inter-satellite data-links can be reliably created. The downlink of data from the complete constellation can therefore be performed twice during every bounce of the constellation.

The deployment of such a constellation using traditional methods would require many launches and would therefore be prohibitively expensive. However, for nanosatellites or picosatellites, the full complement of payloads could be launched by a single launch vehicle.

A sample deployment of a 3U CubeSat constellation with this configuration has been investigated. The properties for this deployment are presented in Table 3. The propulsion system for each satellite in this case has been limited to a maximum Δv of 1 m s^{-1} in every 12 h period. This thrusting performance is well within the capability of microsatellite and nanosatellite propulsion technologies such as miniaturised cold-gas, monopropellant, and bipropellant thrusters [22,46]. For a 3U CubeSat, a propulsion system such as this can be contained within a 1U section.

The results of a sample deployment of a constellation of this configuration are shown in Fig. 8. Only the motion of every 10th satellite in the constellation is shown to maintain clarity. The complete time for deployment of all

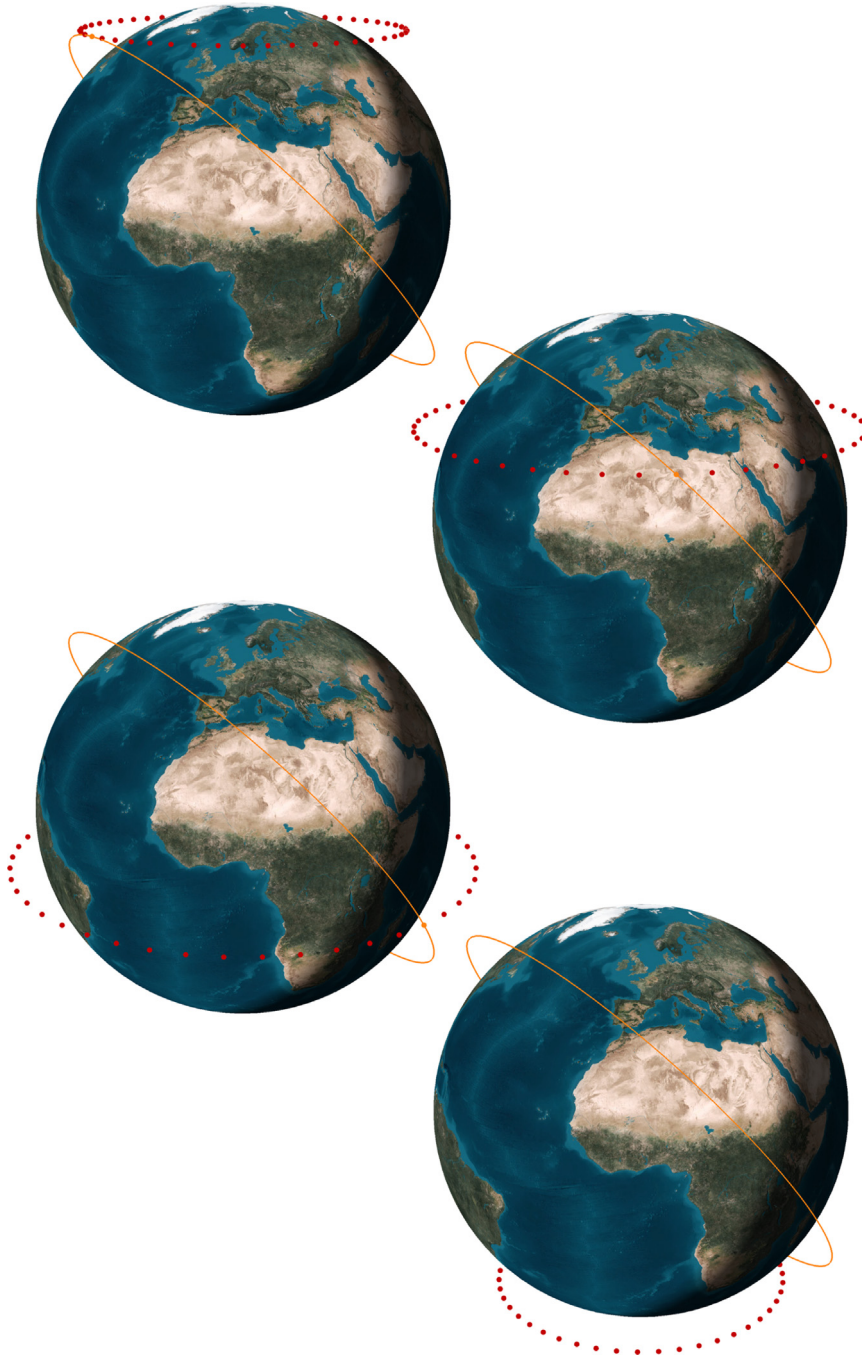


Fig. 7. Halo constellation (60°: 50/50/0).

50 satellites is 47 months, just under 4 years. This is a significant period of time for the deployment phase of a constellation. However, given a greater difference between the initial and mission orbits, the deployment can be executed faster at the expense of additional propulsive requirement.

Due to the high altitude of the insertion orbit for this mission, the satellites do not decay significantly during the drift phases of deployment. The range of Δv required by

the satellites therefore does not vary significantly between the first and last payloads deployed ($87.0\text{--}87.2\text{ m s}^{-1}$).

The deployment of a significant number of very small satellites in a Halo constellation using EML-1 presents a number of significant issues which would prohibit the use of this method for a constellation of this type. The primary issue is due to the configuration of one payload per orbital plane, similar to the deployment of the FORMOSAT-3/COSMIC mission discussed previously.

To perform the Halo ejection and re-circularisation manoeuvres, the propulsive capability of the satellites would have to be increased significantly. For example, the propellant mass required for a satellite of nominal 15 kg dry mass with a propulsion system I_{sp} of 200 s would be 17 kg.

Very small satellites would also require significant system development in order to be capable of performing the aerocapture manoeuvre, requiring highly accurate attitude control and significant heat-shielding due to their typically low thermal inertia. Alternatively, an aerobraking manoeuvre utilising a sail device could be performed. In this case, due to the length of time spent in the Van Allen belts, radiation hardening of components or a fault-tolerant approach to system design would be required, incurring additional development costs or system complexity.

5.3. Global microsatellite constellation

The deployment of a constellation of microsatellites for communications or Earth observation missions can also be

Table 3

Mission properties for Halo constellation.

Property	Value
No. of satellites	50
No. of planes	50
Satellite dry mass	5 kg
Satellite area	0.035 m ²
Satellite C_D	2.2
Insertion orbit	
Semi-major axis, a	7200 km
Eccentricity, e	0.001
Inclination, i	60°
RAAN, Ω	0°
Mission orbit	
Semi-major axis, a_i	7371 km
Eccentricity, e_i	0.001
Inclination, i_i	60°
RAAN	Equispaced about 360°

considered. In this constellation, multiple satellites are required in each orbital plane in order to achieve a certain level of global coverage or minimum revisit time.

The example constellation used has a configuration of six equally spaced planes each containing five payloads at an inclination of 70°. The size and mass of the SSTL Microsat-100 bus, used for the first DMC mission satellites, is used as a reference for the payloads in this study. The constellation and satellite properties for this analysis are shown in Table 4.

The deployment profile of this mission is shown in Fig. 9. Due to the lower initial orbit of the satellites, the decay due to atmospheric drag is considerable, indicated by the decrease in semi-major axis of the payloads in the initial orbit. Over the period of deployment this orbital decay results in the re-entry of the final group of payloads, resulting in the establishment of an incomplete constellation.

To avoid this mission failure, the orbital height of the initial orbit can be increased. Whilst Δv requirement for the in-plane manoeuvre would be reduced, this would result in longer drift periods to achieve the correct plane separations and therefore an extended total time for the deployment of the constellation.

Alternatively, the satellites could be inserted into an orbit with a larger semi-major axis and/or eccentricity than the final mission orbit thus avoiding the issue of decay and increasing the rate of plane separation. However, this may result in greater launch vehicle costs.

Due to the configuration of multiple payloads in each orbital plane, the deployment of this constellation using EML-1 supports the use of carrier vehicles in order to reduce the propulsive requirements for each individual payload. For this deployment, each carrier vehicle can manifest the five payloads specified for each plane.

The carrier vehicle can perform the required Halo orbit injection and ejection manoeuvres at EML-1 and re-circularisation in Earth orbit using a centralised propulsion module. A higher thrust, and greater specific impulse system can be developed due to the lower mass and volume constraints of a system common to the set of

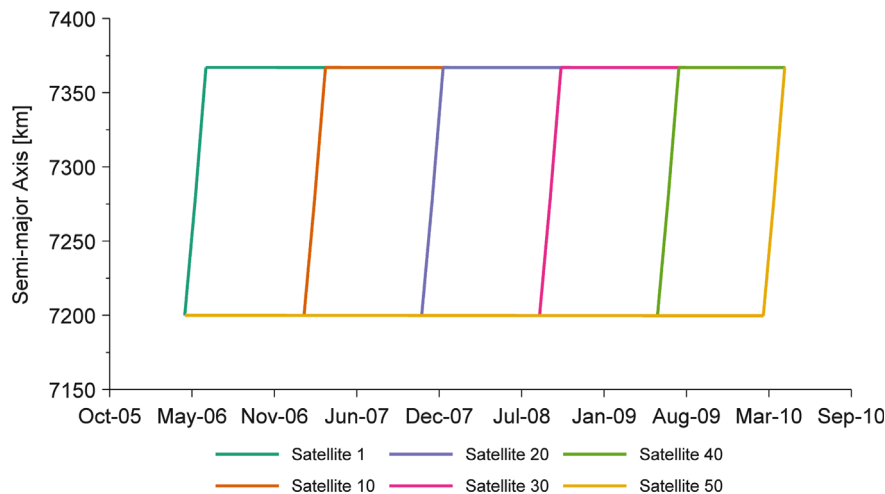


Fig. 8. Semi-major axis of selected satellites through analysed deployment of a sample Halo constellation.

payloads. Once in the required orbital plane, the payloads can be dispensed from the carrier vehicle with varying relative velocities using differential spring energies. The required phasing of the satellites about the orbital plane can thus be achieved with minimal propulsion from each individual payload [28].

Further mass and costs efficiencies can be achieved through the use of carrier vehicles as the high-accuracy ADCS and aerocapture device can be common to the set of satellites whilst also less restricted by the mass and volume of the individual payloads.

For a set of five satellites with a nominal mass of 75 kg, the dry mass of a suitable carrier vehicle can be approximated to 190 kg (50% of payload mass [13]) plus an aerocapture device (ballute) of 100 kg [34]. The additional propellant mass for such a system is calculated to be ~ 405 kg assuming an I_{sp} of 320 s due to the increase in size and capability of the system. A total mass of ~ 1070 kg is subsequently obtained for the mass of each manifested carrier vehicle, resulting in an increase in mass of each original satellite (100 kg) by a factor of 2.1. This is considerably less than the increase in mass previously

determined for the FORMOSAT-3/COSMIC mission in which only a single satellite was required in each plane.

6. Summary

The deployment of constellations using the indirect method of plane separation by differential nodal precession was shown to enable the deployment of a novel type of very small satellite constellation whilst maintaining a low level of propulsive requirement of each payload. However, the drawback of this method was found to be the significant time required to execute the deployment of the payloads over large plane separations. For constellations in low altitude orbits, due to the extended drift periods, the decay of satellites before the deployment has been completed must also be carefully considered. Furthermore, the lifetime of the satellites in orbit following deployment should be investigated to ensure that decay and potential de-orbit does not compromise the mission.

Conversely, the investigation of deployment using EML-1 to dispense satellites into different orbital planes found that this method was most suitable for constellations which require responsive set-up. Due to the significant magnitude of the manoeuvres involved, the propulsive requirements to enable this deployment strategy are much greater than the indirect method. Furthermore, due to the use of aerocapture or aerobraking manoeuvres and multi-payload carrier vehicles to reduce the total and individual payload propulsive requirements, additional system development is needed to enable deployment by this method. For constellations where only a single satellite is required in each orbital plane, this method was found to be inefficient. However, in the analysis of constellations with multiple satellites in each plane, where carrier vehicles could be used effectively to reduce the individual propulsive requirements of the satellites, this method was shown to be more suitable.

Nevertheless, the performed analysis of these different small satellite constellation deployment methods has indicated that the establishment of such systems on a variety of scales in Earth orbit is within the current

Table 4
Mission properties for microsatellite constellation.

Property	Value
No. of satellites	30
No. of planes	6
Satellite dry mass	100 kg
Satellite area	0.975 m ²
Satellite C_D	2.2
Insertion orbit	
Semi-major axis, a	6825 km
Eccentricity, e	0.01
Inclination, i	70°
RAAN, Ω	0°
Mission orbit	
Semi-major axis, a_i	7078 km
Eccentricity, e_i	0.001
Inclination, i_i	70°
RAAN	Equispaced about 360°

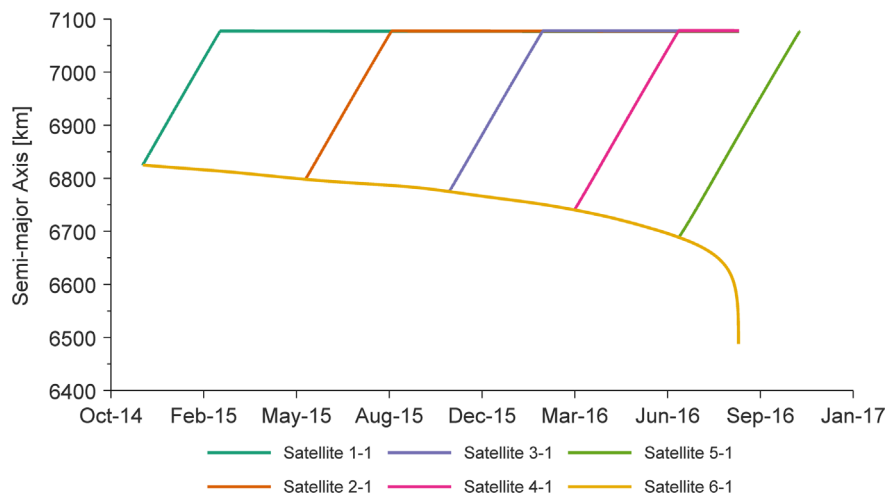


Fig. 9. Semi-major axis and orbit decay profile of microsatellite constellation deployment.

capability of such systems and can be performed using existing payload launch opportunities.

6.1. Future work

Given the relationships between constellation configuration, payload design, and feasibility of deployment shown by the analyses performed, the study of constellation deployment should be performed concurrently throughout the design process to ensure the development of feasible system and mission designs. Currently, these methods of deployment are not considered by existing design processes. The investigation of deployment of small satellite constellations is therefore currently performed on an ad hoc basis without complete analysis. Awareness and knowledge of the solutions to and effects of different constellation deployment strategies may also influence other aspects of the constellation, payload, or platform design resulting in the synthesis of improved overall system or mission designs. The use of design space exploration or optimisation techniques may present a route by which constellation deployment can be investigated and integrated into the system design process.

To more thoroughly investigate the feasibility and potential benefits of constellation deployment using EML-1, an increased understanding of the trajectory design and subsystem requirements and design is required. The development of aerocapture or aerobraking devices for very small satellites and investigation of the aerodynamic effects of these manoeuvres on these satellites may also enable the use of this method for a greater range of mission types.

Acknowledgements

This work was supported by the Doctoral Training Partnership (DTP) between the University of Manchester and the UK Engineering and Physical Sciences Research Council (EPSRC) under grant EP/J50032X/1.

Appendix A. Supplementary data

Supplementary data associated with this article can be found in the online version at <http://dx.doi.org/10.1016/j.actaastro.2015.04.015>.

References

- [1] H.J. Kramer, A.P. Cracknell, An overview of small satellites in remote sensing, *Int. J. Remote Sens.* 29 (15) (2008) 4285–4337, <http://dx.doi.org/10.1080/01431160801914952>. ISSN 0143-1161.
- [2] D. DePasquale, A. Charania, H. Kanayama, S. Matsuda, Analysis of the earth-to-orbit launch market for nano and microsatellites, in: AIAA SPACE 2010 Conference and Exposition, American Institute of Aeronautics and Astronautics (AIAA), Anaheim, CA, 2010.
- [3] G. Webb, A. da Silva Curiel, The changing launcher solutions of the small satellite sector, in: The 62nd International Astronautical Congress, International Astronautical Federation (IAF), Cape Town, SA, 2011.
- [4] K. Woellert, P. Ehrenfreund, A.J. Ricco, H.R. Hertzfeld, Cubesats: cost-effective science and technology platforms for emerging and developing nations, *Adv. Space Res.* 47 (4) (2011) 663–684, <http://dx.doi.org/10.1016/j.asr.2010.10.009>. ISSN 0273-1177.
- [5] F.M. Pranajaya, R.E. Zee, Nanosatellite tracking ships: from concept to launch in 7 months, in: 23rd Annual AIAA/USU Conference on Small Satellites, American Institute of Aeronautics and Astronautics (AIAA), Logan, UT, 2009, pp. 1–6.
- [6] S. Kenyon, C.P. Bridges, STRaND-1: use of a \$500 smartphone as the central avionics of a nanosatellite, in: The 62nd International Astronautical Congress, International Astronautical Federation (IAF), Cape Town, SA, 2011.
- [7] W.L. Nicholson, A.J. Ricco, E. Agasid, C. Beasley, M. Diaz-Aguado, P. Ehrenfreund, C. Friedericks, S. Ghassemieh, M. Henschke, J.W. Hines, C. Kitts, E. Luzzi, D. Ly, N. Mai, R. Mancinelli, M. McIntyre, G. Minelli, M. Neumann, M. Parra, M. Piccini, R. M. Rasay, R. Ricks, O. Santos, A. Schooley, D. Squires, L. Timucin, B. Yost, A. Young, The O/OREOS mission: first science data from the space environment survivability of living organisms (SESLO) payload, *Astrobiology* 11 (10) (2011) 951–958, <http://dx.doi.org/10.1089/ast.2011.0714>. ISSN 1557-8070.
- [8] C. Kitts, J.W. Hines, E. Agasid, A.J. Ricco, B. Yost, K. Ronzano, J. Puig-Suari, The GeneSat-1 microsatellite mission: a challenge in small satellite design, in: The 20th Annual AIAA/USU Conference on Small Satellites, American Institute of Aeronautics and Astronautics (AIAA), Logan, UT, 2006, pp. 1–6.
- [9] J.R. London III, M.E. Ray, D.J. Weeks, A.B. Marley, The first US army satellite in fifty years: SMDC-ONE first flight results, in: The 25th Annual AIAA/USU Conference on Small Satellites, American Institute of Aeronautics and Astronautics (AIAA), Logan, UT, 2011.
- [10] S. Kim, T. Eishima, N. Miyashita, Y. Nojiri, Y. Nakamura, WNISAT—nanosatellite for north arctic routes and atmosphere monitoring, in: The 24th Annual AIAA/USU Conference on Small Satellites, American Institute of Aeronautics and Astronautics (AIAA), Logan, UT, 2010.
- [11] B.T. Patel, S. Schroll, A. Lewin, On-orbit performance of the ORB-COMM spacecraft constellation, in: The 13th Annual AIAA/USU Conference on Small Satellites, American Institute of Aeronautics and Astronautics (AIAA), Logan, UT, 1999.
- [12] C.R. Boshuizen, J. Mason, P. Klupar, S. Spanhake, Results from the Planet Labs Flock constellation in: The 28th Annual AIAA/USU Conference on Small Satellites, American Institute of Aeronautics and Astronautics (AIAA), Logan, UT, 2014.
- [13] J.R. Wertz, W.J. Larson, *Space Mission Analysis and Design*, 3rd ed. Microcosm Press, Kluwer Academic Publishers, El Segundo, CA, 1999 ISBN 978-1-881883-10-4.
- [14] J. Esper, P.V. Panetta, M. Ryschkewitsch, W. Wiscombe, S. Neeck, NASA-GSFC nano-satellite technology for earth science missions, *Acta Astronaut.* 46 (2–6) (2000) 287–296, [http://dx.doi.org/10.1016/S0094-5765\(99\)00214-3](http://dx.doi.org/10.1016/S0094-5765(99)00214-3). ISSN 0094-5765.
- [15] L. Dyrud, S. Slagowski, J. Fentzke, W. Wiscombe, B. Gunter, K. Cahoy, G. Bust, A. Rogers, B. Erlandson, L. Paxton, S. Arnold, Small-sat science constellations: why and how, in: The 27th Annual AIAA/USU Conference on Small Satellites, American Institute of Aeronautics and Astronautics (AIAA), Logan, UT, 2013.
- [16] D.J. Barnhart, T. Vladimirova, M.N. Sweeting, Very-small-satellite design for distributed space missions, *J. Spacecr. Rockets* 44 (6) (2007) 1294–1306, <http://dx.doi.org/10.2514/1.28678>. ISSN 0022-4650.
- [17] D.J. Barnhart, T. Vladimirova, A.M. Baker, M.N. Sweeting, A low-cost femtosatellite to enable distributed space missions, *Acta Astronaut.* 64 (11–12) (2009) 1123–1143, <http://dx.doi.org/10.1016/j.actaastro.2009.01.025>. ISSN 0094-5765.
- [18] R. Sandau, K. Brieß, M. D'Errico, Small satellites for global coverage: potential and limits, *ISPRS J. Photogramm. Remote Sens.* 65 (6) (2010) 492–504, <http://dx.doi.org/10.1016/j.isprsjprs.2010.09.003>. ISSN 0924-2716.
- [19] W.W. Saylor, K. Smaagard, N. Nordby, D.J. Barnhart, New scientific capabilities enabled by autonomous constellations of smallsats, in: The 21st Annual AIAA/USU Conference on Small Satellites, 719, American Institute of Aeronautics and Astronautics (AIAA), Logan, UT, 2007.
- [20] A. da Silva Curiel, M. Lambert, D. Liddle, M.N. Sweeting, C.-H. Chu, C.-J. Fong, G.-S. Chang, Introduction to FORMOSAT-7/COSMIC-2 mission, in: The 27th Annual AIAA/USU Conference on Small Satellites, American Institute of Aeronautics and Astronautics (AIAA), Logan, UT, 2013.
- [21] M. Bille, P. Kolodziejewski, T. Hunsaker, Distant horizons: smallsat evolution in the mid-to-far term, in: The 25th Annual AIAA/USU Conference on Small Satellites, American Institute of Aeronautics and Astronautics (AIAA), Logan, UT, 2011.
- [22] L. Lemmerman, C. Raymond, R. Shotwell, J. Chase, K. Bhasin, R. Connerton, Advanced platform technologies for Earth science, *Acta Astronaut.* 56 (1–2) (2005) 199–208, <http://dx.doi.org/10.1016/j.actaastro.2004.09.031>. ISSN 0094-5765.

- [23] N.H. Crisp, K.L. Smith, P.M. Hollingsworth, Small satellite launch to LEO: a review of current and future launch systems, *Trans. Jpn. Soc. Aeronaut. Space Sci. Aerosp Technol. Jpn.* 12(ists29), ISSN 1884-0485, http://dx.doi.org/10.2322/tastj.12.Tf_39.
- [24] A. Charania, S. Isakowitz, W. Pomerantz, B. Morse, K. Sagis, LauncherOne: revolutionary orbital transport for small satellites, in: *The 27th Annual AIAA/USU Conference on Small Satellites*, vol. 626, American Institute of Aeronautics and Astronautics (AIAA), Logan, UT, 2013.
- [25] K. Rodway, K. Papadopoulos, J. Greason, Utility and application of XCOR's commercial reusable suborbital vehicle Lynx for small satellite launch, in: *The 65th International Astronautical Congress, International Astronautical Federation (IAF)*, Toronto, Canada, 2014.
- [26] C.-J. Fong, C.-Y. Huang, V. Chu, N. Yen, Y.-H. Kuo, Y.-A. Liou, S. Chi, Mission results from FORMOSAT-3/COSMIC constellation system, *J. Spacecr. Rock.* 45 (6) (2008) 1293–1302, <http://dx.doi.org/10.2514/1.34427>. ISSN 0022-4650.
- [27] J. King, N. Beidleman, Method and Apparatus for Deploying a Satellite Network, 1993.
- [28] J. Puig-Suari, G. Zohar, K. Leveque, Deployment of CubeSat constellations utilizing current launch opportunities, in: *The 27th Annual AIAA/USU Conference on Small Satellites*, vol. 805, American Institute of Aeronautics and Astronautics (AIAA), Logan, UT, 2013.
- [29] J.W. Gangestad, B.S. Hardy, D.A. Hinkley, Operations, orbit determination, and formation control of the AeroCube-4 CubeSats, in: *The 27th Annual AIAA/USU Conference on Small Satellites*, American Institute of Aeronautics and Astronautics (AIAA), Logan, UT, 2013.
- [30] R. Rose, W. Wells, J. Redfern, D. Rose, J. Dickinson, C. Ruf, A. Ridley, K. Nave, NASA's Cyclone Global Navigation Satellite System (CYGNSS) mission—temporal resolution of a constellation enabled by microsatellite technology, in: *The 27th Annual AIAA/USU Conference on Small Satellites*, American Institute of Aeronautics and Astronautics (AIAA), Logan, UT, 2013, ISBN 7347646561.
- [31] C.-J. Fong, W.-T. Shiau, C.-T. Lin, T.-C. Kuo, C.-H. Chu, S.-K. Yang, N.-L. Yen, S.-S. Chen, Y.-H. Kuo, Y.-A. Liou, S. Chi, Constellation deployment for the FORMOSAT-3/COSMIC mission, *IEEE Trans. Geosci. Remote Sens.* 46 (11) (2008) 3367–3379.
- [32] J. Chase, N. Chow, E. Gralla, N.J. Kasdin, LEO constellation design using the lunar L1 point, in: *The 14th AAS/AIAA Space Flight Mechanics Meeting*, vol. 609, American Astronautical Society, Maui, HI, 2004.
- [33] M.J. Nadoushan, A.B. Novinzadeh, Satellite constellation build-up via three-body dynamics, *Proc. Inst. Mech. Eng. Part G: J. Aerosp. Eng.* 228 (1) (2014) 155–160, <http://dx.doi.org/10.1177/0954410013476615>, ISSN 0954-4100.
- [34] N. Chow, E. Gralla, N.J. Kasdin, J. Chase, Low Earth Orbit Constellation Design Using the Earth–Moon L1 Point, Technical Report, Princeton University, Princeton, NJ, 2004.
- [35] J. Liu, R. Alford, Semianalytic theory for a close-earth artificial satellite, *J. Guid. Control Dyn.* 3 (4) (1980) 304–311.
- [36] D.A. Vallado, *Fundamentals of Astrodynamics and Applications*, 4th ed. Microcosm Press, Springer, Hawthorne, CA, 2013.
- [37] J. Picone, A. Hedin, D. Drob, A. Aikin, NRLMSISE-00 empirical model of the atmosphere: statistical comparisons and scientific issues, *J. Geophys. Res.* 107(A12), <http://dx.doi.org/10.1029/2002JA009430>, ISSN 0148-0227.
- [38] C. Pardini, L. Anselmo, Comparison and accuracy assessment of semi-empirical atmosphere models through the orbital decay of spherical satellites, *J. Astronaut. Sci.* 49 (2) (2001).
- [39] D. King-Hele, *Satellite Orbits in an Atmosphere: Theory and Applications*, Blackie and Son Ltd, Glasgow, UK, 1987.
- [40] D.A. Vallado, D. Finkleman, A critical assessment of satellite drag and atmospheric density modeling, in: *AIAA/AAS Astrodynamics Specialist Conference and Exhibit*, The American Institute of Aeronautics and Astronautics (AIAA), Honolulu, HI, 2008.
- [41] D.A. Vallado, T. Kelso, Using EOP and space weather data for satellite operations, in: *The 15th AAS/AIAA Astrodynamics Specialist Conference*, American Institute of Aeronautics and Astronautics (AIAA), Lake Tahoe, CA, 2005.
- [42] D.A. Vallado, T. Kelso, Earth orientation parameter and space weather data for flight operations, in: *The 23rd AAS/AIAA Space Flight Mechanics Meeting*, American Institute of Aeronautics and Astronautics (AIAA), Kauai, HI, 2013.
- [43] K. Moe, M.M. Moe, Gas-surface interactions and satellite drag coefficients, *Planet. Space Sci.* 53 (8) (2005) 793–801, <http://dx.doi.org/10.1016/j.pss.2005.03.005>. ISSN 0032-0633.
- [44] D.L. Oltrogge, K. Leveque, An evaluation of CubeSat orbital decay, in: *The 25th Annual AIAA/USU Conference on Small Satellites*, American Institute of Aeronautics and Astronautics (AIAA), Logan, UT, 2011, ISBN 6508594621.
- [45] S.W. Janson, The future of small satellites, in: H. Helvajian, S.W. Janson (Eds.), *Small Satellites: Past, Present, and Future*, The Aerospace Press, El Segundo, CA, 2008 (Chapter 23).
- [46] D.B. Scharfe, A.D. Ketsdever, A review of high thrust, high delta-V options for microsatellite missions, in: *The 45th AIAA Joint Propulsion Conference and Exhibit*, vol. 15, American Institute of Aeronautics and Astronautics (AIAA), Denver, CO, 2009.